



Effect of Hydrogen Addition on Soot Reduction in Diffusion Flames

Lencho Dereje Futassa*, Felix Mwiya†, Wisdom Simwila Kalunga‡, Junior Adolph§, Amit Kumar *||

Department of Aerospace Engineering, Chandigarh University, Chandigarh, India

Abstract: This study explores the effects of hydrogen addition on soot reduction in methane-air diffusion flames, employing computational analysis coupled with chemical equilibrium and k-epsilon combustion turbulence models. By varying the fuel mixture with hydrogen mass percentages ranging from 0% to 11%, alterations in flame behaviour were observed. Results revealed a notable increase in maximum flame temperature at 1.3% hydrogen addition, attributed to enhance combustion efficiency, while subsequent additions led to temperature decrements due to dilution effects. Concurrently, soot production exhibited a general decrease, with reductions quantified up to 96.7% compared to baseline conditions, primarily due to improved oxidation and decreased carbon content. Additionally, the position of maximum flame temperature and soot mass fraction shifted along the axial direction owing to hydrogen's higher flammability compared to methane-air diffusion. These findings offer insights into optimizing flame characteristics for reduced particulate matter emissions, emphasizing the potential of hydrogen addition in mitigating soot formation in diffusion flames.

Table of Contents

1. Introduction.....	1
2. Literature Review.....	2
3. Objectives and Research Methodology.....	2
4. Modelling of Turbulent Non-Premixed Combustion.....	2
5. Numerical Solution.....	5
6. Results and Discussion.....	5
7. Conclusion.....	7
8. References.....	7
9. Acknowledgement.....	8
10. Conflict of Interest.....	8
11. Funding.....	8

1. Introduction

The global community has risen to the task of reducing the climate impacts that are slowly turning habitable earth into a degrading habitat. This has led to a rapid increase in regulations to reduce pollution emissions. Combustion and energy specialists thus face the challenge of finding ways to reduce emissions resulting from combustion. We all need energy; the world needs energy to thrive and prosper. However, if the energy creation process (combustion) is killing us and degrading our habitat, then that energy is not sustainable. We face the problem of soot (black carbon) in the PM range of 2.5, which is warming our globe and causing enormous health problems. It is the duty of everyone, especially combustion and engineering experts, to find more sustainable solutions. From this understanding, we put to the test a method to reduce soot produced during combustion and help the energy sector become less criticized for its effects on health and climate. This research focused on the addition of hydrogen for soot reduction in methane-air non-premixed flames. Our choice of diffusion flame correlates with our knowledge that non-premixed flames are prominent in everyday combustion processes. For example, in industrial burners, diffusion flames are commonly used for furnaces and flares. In rocket engines, we widely use coaxial jet diffusion flames, and in daily life, most fires are indeed diffusion flames. Thus, an analysis involving diffusion flames helps address overall combustion issues applicable to most combustion processes. Methane, a main component of natural gas, was chosen for this study. By analysing methane soot reduction, we can gain a general understanding of soot reduction in natural gas.

*UG Research Scholar, Department of Aerospace Engineering, Chandigarh University, Chandigarh, India. **Contact: 21bas1234@cuchd.in**
 †UG Research Scholar, Department of Aerospace Engineering, Chandigarh University, Chandigarh, India. **Corresponding Author: 21bas1235@cuchd.in**
 ‡UG Research Scholar, Department of Aerospace Engineering, Chandigarh University, Chandigarh, India. **Contact: 21bas1247@cuchd.in**
 §UG Research Scholar, Department of Aerospace Engineering, Chandigarh University, Chandigarh, India. **Contact: 21bas1227@cuchd.in**
 Assistant Professor, Department of Aerospace Engineering, Chandigarh University, Chandigarh, India. **Contact: amit.e14058@cumail.in
 ** Received: 15-June-2024 || Revised: 30-June-2024 || Accepted: 05-July-2024 || Published Online: 07-July-2024.

2. Literature Review

In approaching the research, it was realized that reducing soot formation can be achieved via three mechanisms: chemical aftermath, thermal aftermath, and dilution aftermath. The chemical aftermath (consequence) can be understood by looking at the research undertaken by [Lei Xua et al. \(2020\)](#), where they discovered that H₂ accumulation is more effective than He in decreasing soot formation in ethylene flames due to the chemical inhibition of PAH growth. In methane flames, the effectiveness of H₂ depends on the equivalence ratio. This can be further seen in the study done by [Behzad Rohani et al. \(2021\)](#), where they found that the addition of H₂ reduces the sooting tendency of CH₄ flames. Hydrogen (H₂) significantly influences the creation process of emerging soot particles and results in a reduction in the level of the primary soot precursor, benzene (C₆H₆).

Several methods have been employed to combat combustion emissions, including the purification of fuels and control methods for combustion (e.g., desulphurization, removal of lead in fuels, and the use of exhaust emission control devices that convert toxic gases and pollutants in exhaust gas from an internal combustion engine into less toxic pollutants by catalyzing the redox reaction just ahead of the combustion reaction). Other industry adaptations include lean burning methods (Gasoline Direct Injection and Homogeneous Charge Compression Injection). All these methods have shown significant trends in helping reduce particulate matter (PM 2.5, PM10). In this research, we focused on one aspect of combustion pollution: soot reduction. Soot is a cause of environmental concern due to its impact on health and global warming, as seen in studies by [Ames Hansen et al. \(2004\)](#) and [Osazuwa Clinto et al. \(2023\)](#). Our focus was on soot reduction in methane-air diffusion flames. We were motivated by the need to clean the combustion process and make it more environmentally sustainable, especially since combustion is currently heavily dependent on hydrocarbons and conventional energy sources. We used hydrogen in our approach, as it is said to be the fuel of the future. In our context, we used a hydrogen-hydrocarbon fuel combination to analyze the benefits in terms of soot reduction. The use of hydrogen is attributed to its effect in reducing soot formation or precursors, as shown in the publication by [Liu Fengshan et al. \(2006\)](#).

3. Objectives and Research Methodology

We approached the research with the following objectives:

- To quantify the soot reduction achieved by adding hydrogen to methane-air diffusion flames.
- To elucidate the dominant mechanisms responsible for soot reduction through detailed computational analysis.
- To establish the sooting limits of methane/hydrogen mixtures and compare them to pure methane flames.
- To evaluate the feasibility of using hydrogen-blended fuels for power generation and transportation.

4. Modelling of Turbulent Non-Premixed Combustion

4.1. Turbulence Modeling

The realizable k-epsilon has advantage of predicting the dissipation rate of flow over both flat and round jets accurately over the standard model ([Shaheed et al., 2018](#)). The formula for turbulence is given as following:

$$\frac{\partial}{\partial t}(\rho k) + \frac{\partial}{\partial x_j}(\rho k u_j) = \frac{\partial}{\partial x_j} \left[\left(\mu + \frac{\mu_t}{\sigma_k} \right) \frac{\partial k}{\partial x_j} \right] + G_{kl} - \rho \epsilon - Y_m$$

$$\frac{\partial}{\partial t}(\rho \epsilon) + \frac{\partial}{\partial x_j}(\rho \epsilon u_j) = \frac{\partial}{\partial x_j} \left[\left(\mu + \frac{\mu_t}{\sigma_\delta} \right) \frac{\partial \epsilon}{\partial x_j} \right] - \rho c_2 \frac{\epsilon^2}{k + \sqrt{\nu \epsilon}}$$

The equation (G_k) illustrated below models how the kinetic energy is produced:

$$G_k = -\rho u_t \frac{\partial u_j}{\partial x_j}$$

And u_t herein represents eddy viscosity computed as

$$\mu_t = \rho c_\mu \frac{k^2}{\epsilon}$$

Fluctuating dilation contribution with compressible turbulence in overall dissipation rate is denoted by Y_M and calculated as follows:

$$Y_m = 2\rho\epsilon M_t^2$$

4.2. Combustion Modeling

A chemical equilibrium model simplifies the complexities of turbulent non-premixed combustion. It assumes reactions reach equilibrium at each point within the flow, meaning forward and backward reaction rates are equal. This allows the model to focus on the crucial aspect of mixing between fuel and oxidizer streams, represented by a conserved scalar like mixture fraction. Based on fuel air ratio which is locally and initial temperature, equilibrium calculations determine the final product composition. This model works well for initial assessments and lean flames with simple fuels such as methane which is used in this paper.

And then chemical equilibrium library is integrated with PDF for average scalar quantity calculations.

$$\tilde{\phi} = \int_0^\infty \int_0^1 \phi(Z, x) P(Z, x) dZ dx$$

The equation below in tells the assumption of mixture fraction statistical independence, and the scalar dissipation:

$$P(Z, X) = P(Z)P(X).$$

Scalar dissipation rate mean value is modeled using the following equation:

$$X = C_x \frac{\epsilon}{K} Z''^2$$

where C_x , is taken as a constant and equivalent to 2.5 (Miller & Foster, 2016).

4.3. Radiation Modeling

Accurate modeling of radiative heat transfer in turbulent combustion concerning soot is paramount to understanding intricate flame behavior and pollutant formation. Soot significantly influences radiative heat transfer due to its absorption and emission characteristics across a wide spectrum range. Consequently, there is a need for an accurate representation of soot radiation to avoid significant discrepancies in predicting flame structure and pollutant emissions. The P1 model has been proven to be the superior model for predicting radiative heat transfer in turbulent combustion simulations due to its accuracy (Bestman, 1991).

4.4. Soot Modeling

Soot can be referred to impure carbon particles particularly black, produced when hydrocarbons undergo incomplete combustion. We have three (3) models which we can utilise in the prediction of mass fraction of soot during combustion. Available models we can utilise may include single step model by Khan and Greeves; it does prediction of black particulate (PM) formation rate utilising the simple empirical formula. Secondly, we have two step model proposed by Tesner; it does the prediction of nuclei particles formation including nuclei soot formation. Finally, we have Moss Brookes model for soot prediction which is capable of solving the equations of transport of density of PM number and the mass fraction of soot. There is limited accuracy in the single and two step models. This model has proved to be of better accuracy contrast to the others. Below we have the equations of transport for mass fraction (Y_{soot}) and concentration of radical nuclei (b_{nuc}^*):

$$\frac{\partial}{\partial t}(\rho Y_{soot}) + \nabla \cdot (\rho \vec{v} Y_{soot}) = \nabla \cdot \left(\frac{\mu_t}{\sigma_{soot}} \nabla Y_{soot} \right) + \frac{dM}{dt}$$

$$\frac{\partial}{\partial t}(\rho b_{nuc}^*) + \nabla \cdot (\rho \vec{v} b_{nuc}^*) = \nabla \cdot \left(\frac{\mu_t}{\sigma_{nuc}} \nabla b_{nuc}^* \right) + \frac{1}{N_{norm}} \frac{dN}{dt}$$

Given that,

Y_{soot} = mass fraction of soot (Black Particulate)

M = mass concentration of black particulate in kg/m³

b_{nuc}^* = radical nuclei concentration given by particles x

$$10^{-15}/\text{kg} = \frac{N}{\rho N_{norm}}$$

N = density number of soot particle given by PTC/m³

N_{norm} = 10¹⁵ PTC

The rate of production of soot particles instantaneously can be subjected to nucleation derived from the gas phase and in regime of free molecular coagulation, shown below by the following equation

$$\frac{dN}{d} = C_{\alpha} N_A \left(\frac{X_{prec} P}{RT} \right)^l \exp \left\{ -\frac{T_{\alpha}}{T} \right\} - C_{\beta} \left(\frac{24RT}{\rho_{soot} N_A} \right)^{1/2} d_p^{1/2} N^2$$

where C_{α} , C_{β} and l are taken be model constants. We have, N_A (= 6.022045x10²⁶ kmol⁻¹) as the Avogadro's constant and soot precursor mole fraction denoted by X_{prec} . The soot mass density denoted by ρ_{soot} , has been assumed to be of the value of 1800kg/m³ when the soot particle mean diameter denoted by d_p . Rate of nucleation of soot particles is considered to be proportionate with the concentration of the soot precursor in our case acetylene since we are dealing with methane. Activation temperature denoted by T_{α} for reaction of nucleation have been the work of (Lindstedt, 1994).

Soot mass source term concentration may be given by equation below:

$$\begin{aligned} \frac{dM}{dt} = & M_p C_{\alpha} \left(\frac{X_{prec} P}{RT} \right)^l \exp \left\{ -\frac{T_{\alpha}}{T} \right\} + C_{\gamma} \left(\frac{X_{sgs} P}{RT} \right)^m \exp \left\{ -\frac{T_{\gamma}}{T} \right\} \\ & \left[(\pi N)^{1/3} \left(\frac{6M}{\rho_{soot}} \right)^{2/3} \right]^n - C_{oxid} C_{\omega} \eta_{coll} \left(\frac{X_{oH} P}{RT} \right) \sqrt{T} (\pi N)^{1/3} \left(\frac{6M}{\rho_{soot}} \right)^{2/3} \end{aligned}$$

where C_{γ} , C_{oxid} , C_{ω} , m , and n have been taken to be model constants as well. The constant M_p (= 144kg/kgmol) has been considered to be soot particle mass of incipient, consisting of 12 carbon atoms in our case. Although our assumption makes the model not sensitive to it, surface growth activation requires a greater than zero initial mass. Participating surface growth species mole fraction is denoted by X_{sgs} . Surface addition of gaseous species has been found to grow kerosene soot particles, particularly our precursor i.e. acetylene in abundance has been noticed in non-premixed diffusion flames.

In our model selected it has been assumed that oxidizing agent in dominance in the methane/air diffusion flames is hydroxyl radical and we can utilise the model to formulate the rate of oxidation specifically on the surface of soot by hydroxide radical according to the work of Fennimore and Jones. 0.04 has been assumed to be the collision efficiency denoted by (η_{coll}), given rate of oxidation as concentration soot mass.

We determined the exponents of l , m , n using the work of Moss and Brookes. C_{α} and C_{β} constants can be determined using numerical as a way of modelling for laminar flames in that it can be validated with experimental data.

Below are constants we have utilised in our research according to the work of Moss and Brookes.

C_{α} = 54 s (rate of inception of soot)

T_{α} = 21000 K (soot inception activation temperature)

C_{β} = 1.0 (rate of coagulation)

C_{γ} = 11700kg.m.kmol.s (scaling factor of the rate of surface growth)

$T_\gamma = 12100\text{K}$ (rate of surface growth activation temperature)
 $C_\omega = 105.8125\text{kg.m.kmol.K.s}$ (oxidation constant)
 $\eta_{coll} = 0.04$ (efficiency parameter of collision)
 $C_{oxid} = 0.015$ (rate of oxidation scaling parameter)

5. Numerical Solution

5.1. Computational Domain

Due to the symmetrical nature of the flame, only half of the model was considered. A thorough mesh was created with 829,150 elements, including 10 edge sizing meshes on different edges and one face mesh for the body.

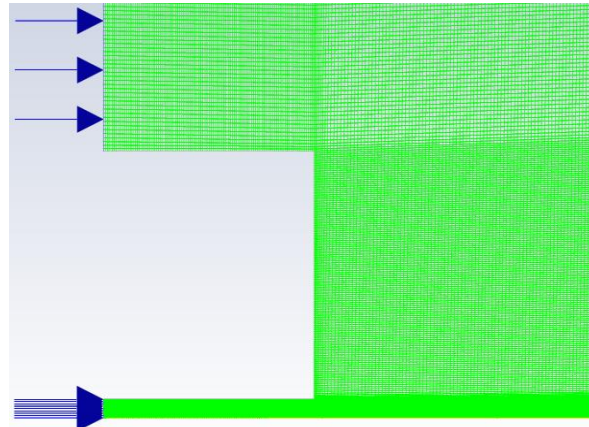


Figure-1 Meshed Inlet of the Model

5.2. Solve Parameters

In this research, the fuel jet velocity is kept constant at 33.4 m/s for all cases. The addition of hydrogen reduces the mass flow rate and density of the fuel because the molecular weight of hydrogen is significantly less than that of the original fuel (methane). Table 1 illustrates the details of all six cases.

5.3. Model Validation and Grid Impedance Study

Solution grid independence was achieved by refining the mesh to the finest mesh with 140,997 cells, particularly focusing on regions with high velocity. These changes were implemented to ensure grid independence, leading to desirable outcomes.

6. Results and Discussion

6.1. Description of Simulation Cases

Six cases are simulated and explained in the results and discussion part of our project. These six cases include the simulation of a pure air-methane diffusion flame in Fluent and the step-by-step addition of hydrogen to the air-methane diffusion flame by both volumetric and mass percentages. This approach allows us to observe how hydrogen addition affects and changes the nature of soot formation, a by-product of combustion resulting in environmental pollution and health problems.

Given the different molecular weights of methane and hydrogen, their volumetric and mass percentages in fuel composition also differ. Hydrogen was added to methane in mass percentages ranging from 0% to 11%. In this simulation, both the fuel inlet velocity (33.4 m/s) and the air inlet velocity (38.2 m/s) were kept constant. Consequently, the density changes over time as the mass percentage of the original fuel changes, in accordance with the mass conservation principle, which states that mass is neither created nor destroyed but remains the same. Table 1 shows all six cases.

Table-1 Six Simulation Cases

Fuel Composition in Volumetric percentage	Fuel Composition in Mass Percentage	Fuel mass flow Rate \times 10^{-4} (kg/s)	Thermal Power \times 10^4 (W)
CH_4	CH_4	2.22	1.110
0.1H₂,0.9CH₄	0.013H ₂ , 0.987CH ₄	2.02	1.033
0.2H₂,0.8CH₄	0.031H ₂ , 0.969CH ₄	1.82	0.949
0.3H₂,0.7CH₄	0.05 H ₂ , 0.95CH ₄	1.64	0.877
0.4H₂,0.6CH₄	0.077H ₂ , 0.923 CH ₄	1.44	0.797
0.5H₂,0.5CH₄	0.11H ₂ , 0.89 CH ₄	1.20	0.692

6.2. Effect of Hydrogen Addition on Flame Temperature

As the temperature of a diffusion flame depends on the fuel composition (mixture ratio), chemical and physical properties of fuels, ambient conditions (air temperature and pressure), and many other factors, changes were observed in the diffusion flame when hydrogen was added to methane. This resulted in significant changes in both flame temperature and soot formation.

With the initial addition of hydrogen, which is 1.3% by mass (0.013) and 10% by volume (0.1), the maximum diffusion flame temperature increased by 0.425% compared to the reference temperature found for a pure methane-air diffusion flame. However, for all other cases, the maximum diffusion flame temperature decreased as the dilution effect outweighed the thermal effect, reducing the overall combustion heat.

One fascinating aspect of this simulation is the shift in the location of the maximum diffusion flame temperature along the axial direction. This shift occurred backward due to the high flammability of hydrogen, which causes faster and earlier combustion than the methane-air diffusion flame without hydrogen addition. This can be explained by the fact that flammability is a chemical property of fuel that indicates how easily a material ignites. Since methane ignites at a higher temperature than hydrogen, the diffusion of a methane-air flame differs from that of a methane-air flame mixed with hydrogen. The more hydrogen is added to methane, the sooner the flame ignites, and thus the shorter the flame becomes, causing the maximum temperature location to shift backward.

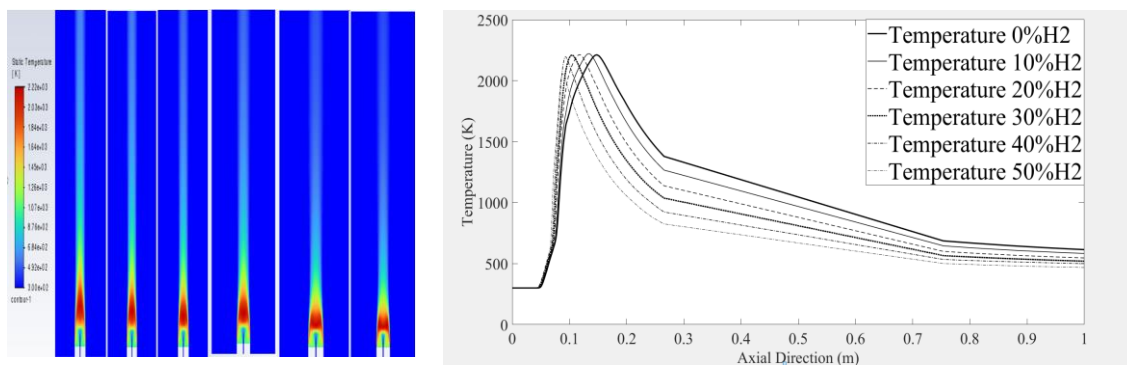


Figure-2 Temperature Contour for 0-50% volumetric Hydrogen added to methane respectively (Left)

Figure-3 Comparison of Temperature for all cases along the axial direction (Right)

Moreover, as the mixture proportion of hydrogen with methane increased, the soot mass fraction decreased, and this trend held true throughout all cases, even if the rate of decrease slowed. An interesting part of the computation is the finding that the length of the axial distance over which soot formation was studied also shrank as the volumetric ratio of hydrogen increased, similar to the shift in the maximum flame temperature location along the axial direction, as shown in the figure below.

6.3. Effect of Hydrogen Addition on Soot Formation

The addition of hydrogen to air-methane fuel in non-premixed combustion (diffusion flame) has resulted in a noticeable change in soot formation and its position along the axial direction. Initially, the computation was performed using only methane as the fuel, with no hydrogen added, and the soot mass fraction was recorded as a reference. When 1.3% mass percentage of hydrogen was added to methane, the soot mass fraction decreased significantly due to the increased maximum temperature, which enhanced the oxidation of hydrocarbons. However, this was true only for the 1.3% mass percentage hydrogen addition, as beyond that point, the maximum temperature decreased. To supplement the table, the results of the simulation were captured as screenshots to provide detailed insights into how the differences appear in the software we used (ANSYS Fluent, the student version). The following figure shows the soot mass fraction contour variations for all six cases, starting from no hydrogen addition to an 11% mass percentage addition to the methane in methane-air diffusion flames. Moreover, as the amount of hydrogen added to methane increased, the soot mass fraction continued to decrease, even though the rate of decrease slowed. An interesting finding of the computation is that the length of the axial distance over which soot formation was studied also shrank as the volumetric ratio of hydrogen increased, similar to the shift in the maximum flame temperature location along the axial direction, as shown in the figure below.

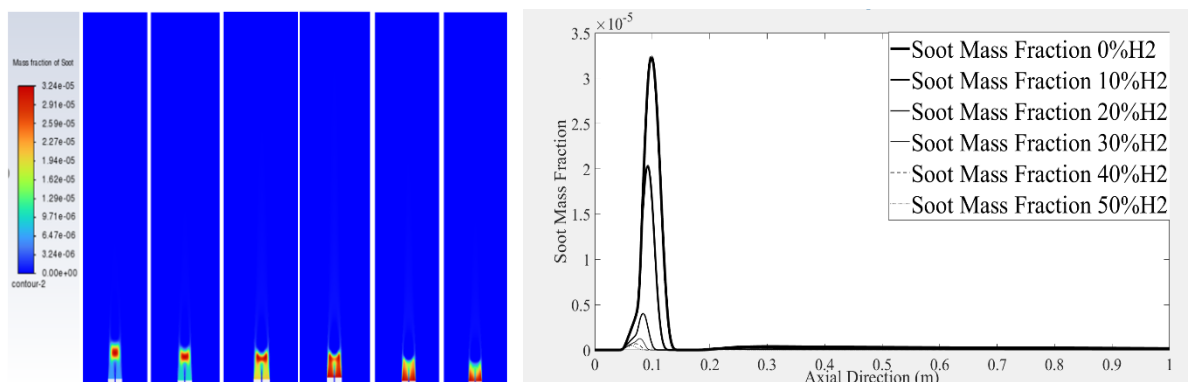


Figure-4 Soot Mass Fraction for 0-50% Volumetric Hydrogen added methane respectively (Left)
Figure-5 Soot Mass Fraction along the axial direction (Right)

7. Conclusion

The computational study focused on the effect of hydrogen addition on soot reduction in methane-air diffusion flames. Six cases ranging from 0% to 11% mass percentage of hydrogen addition were simulated to investigate its impact on soot reduction. As the concentration of hydrogen increased, the soot mass fraction decreased consistently. However, a notable exception was observed with the addition of 1.3% volumetric hydrogen, where the maximum flame temperature increased. Furthermore, the positions of the maximum flame temperature and soot mass fraction were found to shift closer to the axial axis as the hydrogen content increased. This indicates that hydrogen addition not only reduces soot formation but also influences the spatial distribution of temperature and soot within the flame.

8. References

- [1] Blanquart, G., & Pitsch, H. (2009). Analyzing the effects of temperature on soot formation with a joint volume-surface-hydrogen model. *Combustion and Flame*, 156(8), 1614-1626.
- [2] Boyette, W. R., Steinmetz, S. A., Guiberti, T. F., Dunn, M. J., Roberts, W. L., & Masri, A. R. (2021). Soot formation in turbulent flames of ethylene/hydrogen/ammonia. *Combustion and Flame*, 226, 315-324.
- [3] Busupally, M. R., & De, A. (2016). Numerical modeling of soot formation in a turbulent C₂H₄/air diffusion flame. *International Journal of Spray and Combustion Dynamics*, 8(2), 67-85.
- [4] Ekhtator, O. C., Orish, F. C., Nnadi, E. O., Ogaji, D. S., Isuman, S., & Orisakwe, O. E. (2023). Impact of black soot emissions on public health in Niger Delta, Nigeria: Understanding the severity of the problem. *Inhalation Toxicology*, 1–13. <https://doi.org/10.1080/08958378.2023.2297698>
- [5] Franzelli, B., Cuoci, A., Stagni, A., Ihme, M., Faravelli, T., & Candel, S. (2017). Numerical investigation of soot-flame-vortex interaction. *Proceedings of the Combustion Institute*, 36(1), 753–761.
- [6] Guo, H., Liu, F., Smallwood, G. J., & Gülder, Ö. L. (2006). Numerical study on the influence of hydrogen addition on soot formation in a laminar ethylene-air diffusion flame. *Combustion and Flame*, 145(1–2), 324–338. <https://doi.org/10.1016/j.combustflame.2005.10.016>
- [7] Hansen, J. E., & Nazarenko, L. (2003). Soot climate forcing via snow and ice albedos. *Proceedings of the National Academy of Sciences of the United States of America*, 101(2), 423–428. <https://doi.org/10.1073/pnas.2237157100>

-
- [8] Haynes, B. S., & Wagner, H. G. (1981). Soot formation. *Progress in Energy and Combustion Science*, 7(4), 229–273. [https://doi.org/10.1016/0360-1285\(81\)90001-0](https://doi.org/10.1016/0360-1285(81)90001-0)
- [9] Khare, R., Vlavakis, P., Von Langenthal, T., Loukou, A., Khosravi, M., Krämer, U., & Trimis, D. (2022b). Experimental investigation of the effect of hydrogen addition on the sooting limit and structure of methane/air laminar counterflow diffusion flames. *Fuel*, 324, 124506. <https://doi.org/10.1016/j.fuel.2022.124506>
- [10] Lindstedt, P. R. (1994). Simplified soot nucleation and surface growth steps for non-premixed flames. In *Soot formation in combustion: Mechanisms and models* (pp. 417-441). Berlin, Heidelberg: Springer Berlin Heidelberg.
- [11] Liu, F., Ai, Y., & Kong, W. (2014). Effect of hydrogen and helium addition to fuel on soot formation in an axisymmetric coflow laminar methane/air diffusion flame. *International Journal of Hydrogen Energy*, 39(8), 3936-3946.
- [12] Liu, A. (2020). Population balance modelling of soot formation in laminar flames (Doctoral dissertation, Imperial College London).
- [13] Miller, R. S., & Foster, J. (2016). Survey of turbulent combustion models for large-eddy simulations of propulsive flowfields. *AIAA Journal/AIAA Journal on Disc*, 54(10), 2930–2946. <https://doi.org/10.2514/1.j054740>
- [14] Rohani, B., & Saqr, K. M. (2012). Effects of hydrogen addition on the structure and pollutant emissions of a turbulent unconfined swirling flame. *International Communications in Heat and Mass Transfer*, 39(5), 681-688.
- [15] SAUFI, A. E. (2016). Soot formation and evolution in a laminar diffusion flame perturbed by a line vortex. A focus on the impact of unsteady effects on complex chemistry.
- [16] Shaheed, R., Mohammadian, A., & Kheirkhah Gildeh, H. (2019). A comparison of standard $k-\epsilon$ and realizable $k-\epsilon$ turbulence models in curved and confluent channels. *Environmental Fluid Mechanics*, 19, 543-568.
- [17] Wang, C. (2020). The development and implementation of a population balance method-based soot model in diffusion flames (Doctoral dissertation, UNSW Sydney).
- [18] Wang, H. (2011). Formation of nascent soot and other condensed-phase materials in flames. *Proceedings of the Combustion Institute*, 33(1), 41-67.
- [19] Wu, L., Kobayashi, N., Li, Z., & Huang, H. (2016). Experimental study on the effects of hydrogen addition on the emission and heat transfer characteristics of laminar methane diffusion flames with oxygen-enriched air. *International Journal of Hydrogen Energy*, 41(3), 2023-2036.
- [20] Wu, R., Song, X., Wei, J., Bai, Y., Wang, J., Lv, P., ... & Yu, G. (2024). Hydrogen addition in methane-oxygen laminar inverse diffusion flames: A study focused on free radical chemiluminescence and soot formation. *International Journal of Hydrogen Energy*, 54, 1029-1039.
- [21] Xu, L., Yan, F., Wang, Y., & Chung, S. H. (2020). Chemical effects of hydrogen addition on soot formation in counterflow diffusion flames: Dependence on fuel type and oxidizer composition. *Combustion and Flame*, 213, 14-25.

9. Acknowledgement

We would like to thank our supervisor **Dr. Amit Kumar** for his continuous guidance and support in the completion of this project.

10. Conflict of Interest

The author declare no competing conflict of interest.

11. Funding

No funding was received to support this study.
